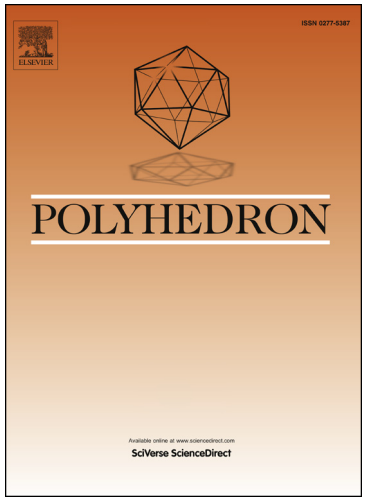

A new near-IR luminescent erbium(III) complex with potential application in OLED devices

Pablo Martín-Ramos, Micael D. Miranda, Manuela Ramos Silva, M. Ermelinda S. Eusebio, Víctor Lavín, Jesús Martín-Gil

PII: S0277-5387(13)00598-6
DOI: http://dx.doi.org/10.1016/j.poly.2013.08.035
Reference: POLY 10295

To appear in: *Polyhedron*

Received Date: 4 June 2013
Accepted Date: 9 August 2013

Please cite this article as: P. Martín-Ramos, M.D. Miranda, M.R. Silva, M. Ermelinda S. Eusebio, V. Lavín, J. Martín-Gil, A new near-IR luminescent erbium(III) complex with potential application in OLED devices, *Polyhedron* (2013), doi: http://dx.doi.org/10.1016/j.poly.2013.08.035

A new near-IR luminescent erbium(III) complex with potential application in OLED devices

Pablo Martín-Ramos[a*], Micael D. Miranda[b], Manuela Ramos Silva[b], M. Ermelinda S. Eusebio[c], Víctor Lavín[d], Jesús Martín-Gil[e]

[a] Higher Technical School of Telecommunications Engineering, Universidad de Valladolid, Campus Miguel Delibes, Paseo Belén 15, 47011 Valladolid, Spain. Tel: +34629022607; E-mail: pablomartinramos@gmail.com

[b] CEMDRX, Physics Department, Universidade de Coimbra, Rua Larga, P-3004-516 Coimbra, Portugal.

[c] Chemistry Department. Faculdade de Ciências e Tecnologia, Universidade de Coimbra, P-3004-535 Coimbra, Portugal.

[d] MALTA Consolider Team, and Department of Fundamental and Experimental Physics, Electronics and Systems, Universidad de La Laguna, E-38200 San Cristóbal de La Laguna, Santa Cruz de Tenerife, Tenerife, Spain

[e] Advanced Materials Laboratory, ETSIIAA, Universidad de Valladolid, Avenida de Madrid 44, 34004 Palencia, Spain

Abstract

We report the synthesis and X-ray structural characterization of the new Er^{3+} ternary complex $[Er(hd)_3(bipy)]$ (where Hhd is 3,5-heptanedione and bipy is 2,2'-bipyridine) as well as its absorption/luminescent properties. X-ray analysis of the novel complex reveals its triclinic centrosymmetric structure with two symmetry independent complexes in the unit cell. Each lanthanide ion is surrounded by 6 oyxgen atoms and 2 nitrogen atoms in a square antiprismatic geometry. The solid-state electronic absorption spectra and the luminescence spectrum show long-wavelength 4f–4f transitions which provide a potential use of the compound as a NIR emitting material in organic light-emitting devices (OLEDs).

Keywords: erbium(III), β-diketonate, photoluminescence

1. Introduction

Nowadays lanthanide(III) complexes with organic ligands present a promising class of emissive materials for organic light-emitting diodes (OLEDs) [1,2]. The unique properties of lanthanide(III) ions arise from their electronic configuration with many spectroscopic terms and energetically close f-levels. Moreover, the energy distances between respective levels give a combination suitable for many up and down conversion processes and some Ln(III) complexes exhibit narrow-line emission in the near infrared range. These properties make them suitable for potential applications in telecommunications, electronics, detector technology, biomedical analysis and medicine, as well as in security and defense [3]. However, the number of reliable near-IR luminescent lanthanide complexes available today for OLED devices is negligible [4]. In previous studies [5,6] we have shown that Er(III) fluorinated β-diketonate complexes with N,N-donors can be used for low cost solution processed OLEDs, since such compounds show good processability and thin film forming properties. For NIR-OLED prototypes based on an analogous complex with 5-nitro-1,10-phenanthroline [6], we demonstrated that –upon excitation with an applied voltage- there was IR emission at 1.54 μm and a total quenching of the visible emission. In this work we describe a new ternary erbium(III) complex with ligands 3,5-heptanedione and 2,2'-bipiridine. The singlet and triplet excited state energies of these ligands exceed those of several NIR excited states of Er^{3+} ion and are suitable to achieve an efficient metal-centered NIR emission. This makes the novel complex a promising candidate as a NIR light-emitting material for OLEDs.

2. Experimental

2.1. *Materials*

All reagents and solvents employed were commercially available and used as supplied without further purification. All the procedures for complex preparation were carried out under nitrogen environment and using dry reagents to avoid the presence of water and oxygen, which can quench erbium photoluminescence.

2.2. *Synthesis*

Tris(3,5-heptanedionate)mono(2,2-bipyridine)erbium(III), [Er(hd)$_3$(bipy)], was obtained as follows: under stirring, a 3,5-heptanedionate (3 mmol) methanol solution (20 ml) was added to 1 mmol of $Er(NO_3)_3 \cdot 5H_2O$ in methanol. The mixture was neutralized by adding potassium methoxide (3 mmol) dropwise under vigorous stirring until potassium nitrate precipitated. KNO_3 was removed by decanting, and 2,2'-bipyridine (1 mmol) was finally added. The mixture was heated to 75ºC and stirred overnight, then washed with dioxane, and finally dried in vacuum to give product in 90-95% yield (based in Er). Crystals suitable for X-ray analysis were obtained by slow evaporation of a methanol-dioxane solution at RT.

[Er(hd)$_3$(bipy)]: Chemical formula: $C_{31}H_{41}ErN_2O_6$, M_W: 704.92. Anal. Calcd. for $C_{31}H_{41}ErN_2O_6$: C, 52.82; H, 5.86; Er, 23.73; N, 3.97; O, 13.62. Found: C, 52.83; H, 5.81; N, 3.92.

2.3. *Physical and optical measurements*

C, H, N elemental analyses were made using a Perkin Elmer CHN 2400 apparatus.

Differential scanning calorimetry (DSC) data were obtained on a DSC Pyris1 Perkin Elmer instrument, equipped with an intracooler cooling unit at -25 ºC (ethylenglycol-water, 1:1 v/v, cooling mixture), with a heating rate β=10°C/min, under a N_2 purge, 20 mL/min. Samples were hermetically sealed in aluminium pans, and an empty pan was used as a reference. Temperature calibration was performed with high-grade standards, biphenyl (CRM LGC 2610) and indium (Perkin-Elmer, x=99.99%), which was also used for enthalpy calibration [7,8].

The infrared spectrum was recorded with a Thermo Nicolet 380 FT-IR apparatus by the use of KBr pellet method.

The Raman spectrum was recorded by a FT-Raman Bruker FRA106 by using a near-IR (Nd: YAG, 1064.1 nm) laser to excite the sample.

The crystal structure was elucidated by X-ray diffraction analysis. Prior to structural characterisation, the powder diffractogram of the erbium complex was obtained. A glass capillary was filled with powder obtained by grinding the solid. The sample was mounted on an ENRAF-NONIUS powder diffractometer (equipped with a CPS120 detector by INEL) in a Debye-Scherrer geometry. Cu Kα radiation was used (λ=1.540598 Å). Silicon was used as an external calibrant.

For the determination of crystal structure by x-ray diffraction, a crystal of [Er(hd)$_3$(bipy)] was glued to a glass fibre and mounted on a Bruker APEX II diffractometer. Diffraction data was collected at room temperature 293(2) K using graphite monochromated MoKα (λ=0.71073 Å). Absorption corrections were made using SADABS [9]. The structure was solved by direct methods using SHELXS-97 [10] and refined anisotropically (non-H atoms) by full-matrix least-squares on F^2 using the SHELXL-97 program [10]. For the terminal methyl a disorder model had to be used allowing two positions for each CH_3. For the carbon atoms that share these methyl groups, it was required to restrain the C-C distances by using DFIX instructions. PLATON [11] was used to analyse the structure and for figure plotting. The

crystallographic details and selected interatomic distances and angles are given in Table 1 and Table 2, respectively.

The optical absorption spectrum of the product in the UV-Vis region was recorded with a Shimazdu UV-2450 UV-Vis spectrophotometer. The visible photoluminescence spectrum was excited with a 280 nm laser diode, and collected with a 0.303 focal length Shamrock spectrometer with Andor Newton cooled CCD camera. The ligand lifetimes have been measured using an Edinburgh Instruments LifeSpec II fluorescence spectrometer, exciting the complex at λ=280 nm with an Edinburgh Instruments EPLED-280 picosecond pulsed LED (temporal pulse width of less than 950 ps), and using Edinburg Instruments F900 acquisition software. The NIR photoluminescence spectrum was excited at the ligands absorption at around 337 nm with a N_2 laser. NIR photoluminescence time decay measurements were excited at 980 nm resonantly with the $^4I_{15/2} \rightarrow {}^4I_{11/2}$ transition of the Er^{3+} ions with an OPO (EKSPLA NT 342/3/UVE). The NIR luminescence was analyzed with a Peltier-cooled InGaAs Hamamatsu pin photodiode G5851-21 at -25ºC and a Horiba Jobin Yvon Triax 180 monochromator. Lifetimes were measured by using a Tektronix (model 3840) oscilloscope. All the spectra have been measured at room temperature and have been corrected by the spectral response of the experimental setups. and samples were analysed directly as powder.

3. Results and discussion

3.1. *Structural description*

$[Er(hd)_3(bipy)]$ crystallizes in a triclinic centrosymmetric cell with four complexes per unit cell, out of which two of them are symmetry independent (Figure 1, Table 1). Within each complex, the lanthanide Er(III) ion is eight-coordinated with N and O neighbours forming a square antiprismatic structure. For the Er1 complex the set N1A, N2A, O1B, O2B and the set O1A, O2A, O1C, O2C form two approximate squares, respectively (Figure 1). In the center of the antiprism lies the trivalent erbium with a distance of 1.3643(2) Å to the face containing the N atoms and 1.1934(2) Å to the opposite face containing exclusively oxygen atoms. Similarly, for the Er2 complex, the set N1B, N2B, O1D, O2D and the set O1E, O2E, O1F, O2F form two approximates squares, respectively (Figure 1). In the center of the antiprism lies the trivalent erbium with a distance of 1.3860(2) Å to the face containing the N atoms and 1.1836(2) Å to the opposite face containing exclusively oxygen atoms.

The Er1-N distances are 2.542(3) Å and 2.537(3) Å and the Er1-O distances are in the range of 2.260(2)- 2.302(3) Å. The Er2-N distances are 2.550(3) Å and 2.557(3) Å and the Er2-O distances are in the range 2.281(3)- 2.321(3) Å. The bite angle N-Er1-N is 62.50(9)º and the bite angle N-Er2-N is 62.47(11)º (Table 2).

The aromatic rings of the 2,2'-bipyridine do not share the same plane. For the Er1 complex, the least-squares plane of the ring that contain the N1A makes a dihedral angle of 7.7(2)° with the least-squares plane of the ring containing N2A. In the Er2 complex, those two least-squares planes, defined by the rings that contain N1B and N2B respectively, make a dihedral angle of 12.4(2)°.

Table 1. Crystal data and structure refinement parameters

Complex	$[Er(hd)_3(bipy)]$
Empirical formula	$C_{31}H_{41}ErN_2O_6$
Formula weight	704.92
Temperature (K)	293(2)
Wavelength (Å)	0.71073
Crystal system	Triclinic
Space group	*P-1*

a (Å)	10.2331(5)
b (Å)	15.8663(8)
c (Å)	21.5723(11)
α (°)	82.185(3)
β (°)	79.555(3)
γ (°)	73.638(3)
Volume (Å^3)	3291.6(3)
Z	4
Calculated density (g/cm^3)	1.422
Absorption coefficient (mm^{-1})	2.590 mm^{-1}
F(000)	1428
Crystal size (mm^3)	0.40×0.10×0.05 mm^3
θ range for data collection (°)	1.34-25.95
Index ranges	-12<h<12; -19<k<19; -26<l<26
Reflections collected/unique (R_{int})	46851/12677 (0.0475)
Completeness to θ = 25°	98.4%
Refinement method	Full matrix LS on F^2
Data/restrains/parameters	12677/26/731
Goodness-of-fit on F^2	1.001
Final R indices [I>2σ(I)]	R_1=0.0386; wR_2=0.0843
R indices (all data)	R_1=0.0798; wR_2=0.1005
Largest difference in peak and hole (e Å^{-3})	-0.456 /0.650

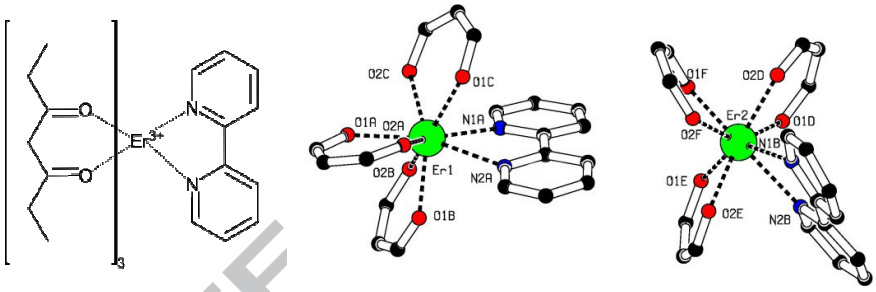

Figure 1. Chemical structure (*left*) and structural diagram (*right*) of two independent [Er(hd)$_3$(bipy)] complexes, showing the antisquare prismatic conformation (H atoms and terminal C atoms were omitted for clarity).

Table 2. Selected bond lengths (Å) and angles (°) at room temperature

Bond	Er1	Bond	Er2
Er1-O1A	2.260(2)	Er2-O1D	2.292(3)
Er1-O2A	2.302(3)	Er2-O2D	2.281(3)
Er1-O1B	2.289(2)	Er2-O1E	2.282(3)
Er1-O2B	2.273(3)	Er2-O2E	2.321(3)
Er1-O1C	2.285(3)	Er2-O1F	2.301(3)
Er1-O2C	2.297(2)	Er2-O2F	2.297(3)
Er1-N1A	2.542(3)	Er2-N1B	2.550(3)
Er1-N2A	2.537(3)	Er2-N2B	2.557(3)
N1A···Er1···N2A	62.50(9)	N1B···Er2···N2B	62.47(11)
N1A···Er1···O2B	73.93(10)	N1B···Er2···O2D	71.55(10)
N1A···Er1···O2C	78.07(9)	N1B···Er2···O2E	74.37(10)
N2A···Er1···O1B	73.85(9)	N2B···Er2···O1D	73.54(9)
N2A···Er1···O1C	71.14(10)	N2B···Er2···O1E	83.64(10)
O1A···Er1···O2A	73.23(10)	O1D···Er2···O2D	74.30(10)
O1B···Er1···O2B	73.77(9)	O1E···Er2···O2E	73.77(10)
O1C···Er1···O2C	72.95(10)	O1F···Er2···O2F	74.14(10)

O1A···Er1···O2B	78.39(10)	O1D···Er2···O1F	82.33(9)
O1A···Er1···O2C	75.47(9)	O1E···Er2···O1F	75.98(10)
O1B···Er1···O2A	76.07(10)	O2E···Er2···O2F	74.68(9)
O1C···Er1···O2A	75.15(11)	O2D···Er2···O2F	79.64(9)

There are signs of disorder in the structure: some terminal methyl groups of 3,5-heptanedionate exhibit a large displacement factor. For both complexes, and for each ligand, two positions could be found for each terminal group that were refined isotropically. Terminal C-C distances were constrained to be 1.50±0.03 Å(Figure 2).

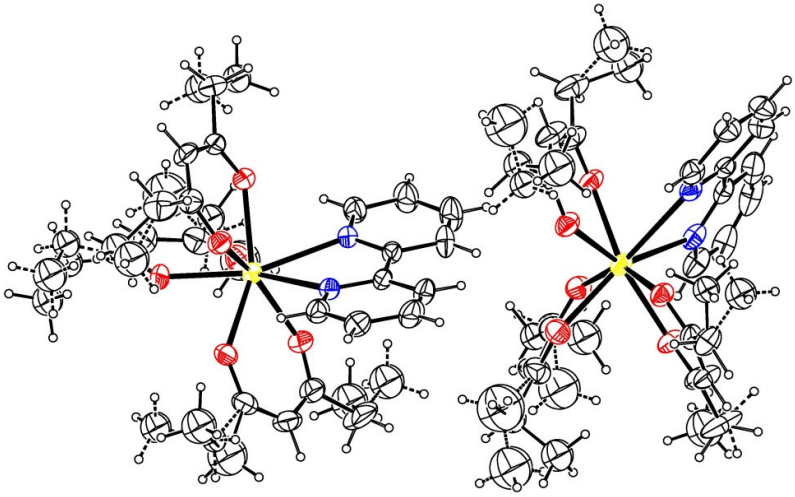

Figure 2. ORTEP plot of two independent [Er(hd)$_3$(bipy)] complexes. For clarity, displacement ellipsoids are drawn at the 20% level.

3.2. *X-ray powder diffraction*

Figure 3 shows the experimental diffraction pattern and the simulated powder pattern from the single crystal structure using PLATON [11]. There is an excellent match between the simulated and the experimental diffractograms: the peaks appear at the predicted theta angles at the same relative intensities. The experimental diffractogram shows a background higher for low theta angles as expected from the diffuse scattering of X-rays by glass and air, a common characteristic when using rotating capillaries in a Debye-Scherrer geometry. Powder diffraction shows that all the material synthesized contains the same structure as the small single crystals used for single-crystal X-ray diffraction.

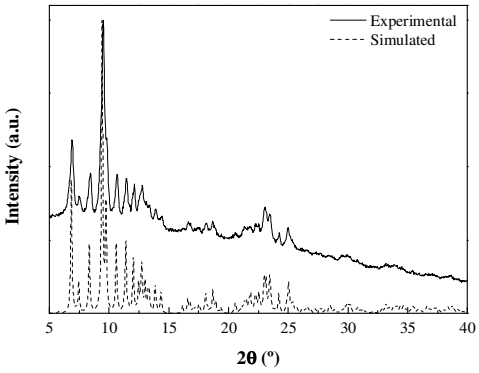

Figure 3. Experimental (*solid line*) *vs.* simulated (*dashed line*) X-ray powder diffraction pattern for [Er(hd)$_3$(bipy)]

3.3. *Differential scanning calorimetry*

Figure 4 shows three heating curves, mediated by two cooling cycles, for [Er(hd)$_3$(bipy)]. In the first heating run, a complex melting peak is observed with onset and peak temperature values T_{onset}=146 ºC and T_{peak}=150 ºC, respectively, and $\Delta_{fus}H$=54 J/g. Crystallization takes place upon cooling with a significant undercooling (about 55 ºC). In the subsequent heating run, the observed peak is broader, with T_{onset}=136 ºC, T_{peak}=146 ºC and $\Delta_{fus}H$=43 J/g. Crystallization still occurs, even at a higher cooling rate, as it is shown in the second cooling run (Figure 4). In the third heating run, the onset and peak temperatures are further lowered to T_{onset}=131 ºC and T_{peak}=142 ºC, as well as the fusion enthalpy, $\Delta_{fus}H$=39 J/g, and the peak gets even broader. This behavior is consistent with some degradation process taking place upon fusion.

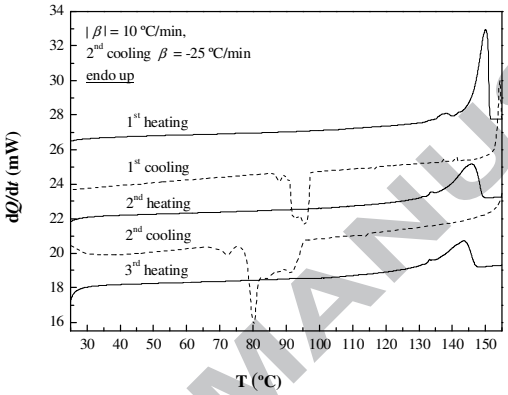

Figure 4. DSC heating/cooling cycles for [Er(hd)$_3$(bipy)], performed at |β|=10 ºC/ min, except for the 2nd cooling run (β=-25 ºC/min), mass m=2.69 mg.

3.4. *FTIR spectroscopy*

The IR spectrum of the complex (Figure 5) shows the expected absorption bands for the β-diketonate ligand and the N,N-donor molecules. The absorption bands have been identified in accordance with the literature [12]. The bands assigned to ring stretching modes CN, CC_{str} (B_1 symmetry) and C=O, and ring 'breathing' modes are observed in the range 1617-1516 cm^{-1} and 1012 cm^{-1}, respectively. They are shifted in comparison with those of the free ligands, suggesting that they are coordinated to erbium(III) [13].

The IR spectrum of the complex under 900 cm^{-1} exhibits the absorption bands at 642, 739 and 770 cm^{-1} characteristic for N,N-donor ligand 2,2'-bipyridine. The band at 739 cm^{-1} is attributed to a ring breathing mode of the 2,2'-bipyridine ligand.

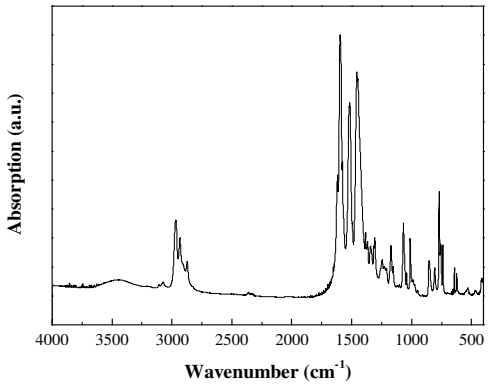

Figure 5. FTIR spectrum of $[Er(hd)_3(bipy)]$

3.5. *Raman spectroscopy*

In the region around 1600 cm^{-1} the complex shows C=O stretching frequencies shifted from those of the β-diketonate free ligand, thus providing good evidence of the fact that the lanthanide ion is coordinated through the oxygen atoms. The peak at around 1450 cm^{-1}, assigned to C=N ring vibrations, and the vibrational mode at around 780 cm^{-1}, assigned to CH out-of-plane for the N,N-donor in the complex, are also shifted from those which appear in its respective free ligand spectra, giving evidence of the fact that nitrogen atoms are coordinated to Er^{3+}. Finally, the Raman-active peak at 400 cm^{-1} is assigned to νEr-N modes.

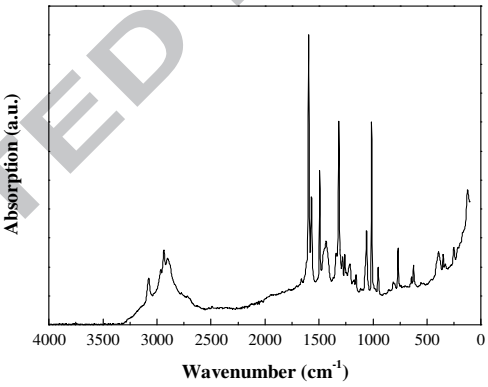

Figure 6. Raman spectrum of $[Er(hd)_3(bipy)]$

3.6. *UV-Vis absorption*

Figure 7 shows the absorption spectrum of $[Er(hd)_3(bipy)]$ complex in methanol diluted solutions. The broad absorption bands in the range from 200 to 370 nm observed at 10^{-5}M can be assigned to the electronic transitions from the ground-state level (π) S_0 to excited level (π^*) S_1 of the organic ligands. The lowest transition (0-0) occurs at 3.22 eV (385 nm), while the main absorption peak is shifted 1.03 eV, at 4.25 eV (292 nm), indicating that the atomic configuration of the excited state is different from that corresponding to the ground state of the molecule.

Above 370 nm, the sharp f-f transitions of Er^{3+} appear: in the same Figure 7 and overlapping the ligand absorption onset it is possible to observe the one corresponding to $^4I_{15/2} \rightarrow {}^4G_{11/2}$ (380 nm) Er states and, by increasing the concentration up to 10^{-3}M (inset in

Figure 7, 450-700 nm region), those corresponding to the transitions from the fundamental $^4I_{15/2}$ Er state to $^4F_{7/2}$ (488 nm), $^2H_{11/2}$ (520 nm), $^4S_{3/2}$ (544 nm) and $^4F_{9/2}$ (655 nm) Er states can also be clearly discerned [14]. The most intense transition corresponds to $^4I_{15/2}\rightarrow{}^2H_{11/2}$ at 520 nm, which is a hypersensitive transition [14] and its intensity is inversely related to the symmetry in the coordination sphere of the lanthanide (i.e., the higher intensity, the lower the symmetry in the coordination sphere) [15].

Absorption spectrum of the $[Er(hd)_3(bipy)]$ complex in the 800-1100 nm (NIR) region (not shown) measured in KBr pellets shows a main band set associated to $^4I_{15/2}\rightarrow{}^4I_{11/2,13/2}$ transitions at 978 nm.

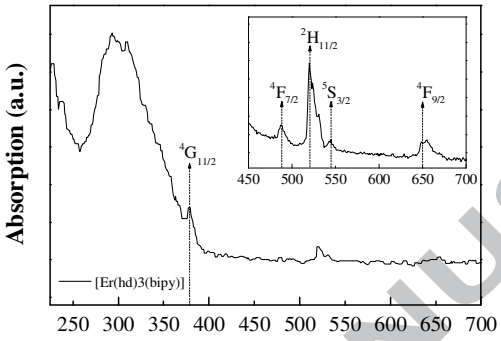

Figure 7. UV-Vis absorption spectra (220-700 nm), (*inset*) zoom-in (450-700 nm region)

3.7. *Photoluminescence in solid state*

Visible photoluminescence emission

The emission of the novel Er^{3+} complex in the visible region (320-750 nm) has been studied under direct excitation of the organic ligands at λ_{exc}=280 nm (Figure 8). The organic part of the complex exhibits a maximum at 386 nm and a shoulder at 458 nm. The former can be tentatively attributed to coordinated Hhd, and the later to coordinated bipy. Since the emission spectrum has been measured in powder, it is expected that it may be slightly red-shifted in comparison to that obtained in solution, as a result of the aggregation state.

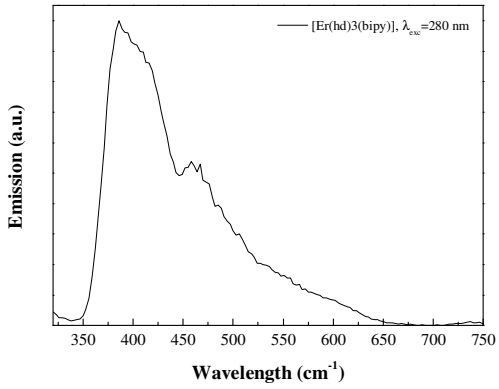

Figure 8. PL spectrum in the visible region

Infrared photoluminescence emission

Excitation of the organic ligands at λ=337 nm led to infrared luminescence at λ=1532 nm, associated to the $^4I_{13/2} \rightarrow {}^4I_{15/2}$ transition of trivalent erbium ion (Figure 9). This is the so-called *antenna effect*: under this direct excitation, ground state absorption $S_0 \rightarrow S_1$ in the ligand moiety occurs, followed by fast vibrational relaxation to the lowest excited singlet level, from which it can relax radiatively emitting a photon at around 420 nm or it may undergo intersystem crossing (ISC) to the triplet level due to spin reorientation, from which subsequent resonant energy transfer (ET) to Er^{3+} takes place (Figure 10).

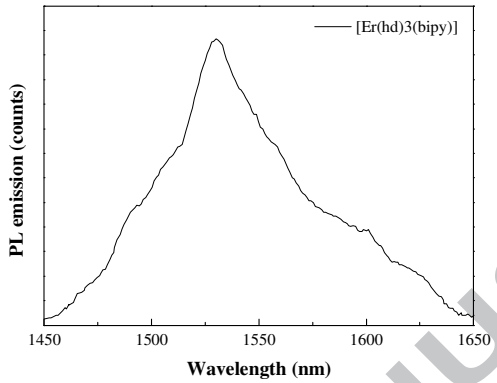

Figure 9. NIR PL spectrum upon excitation of the organic ligands in the UV (λ=337 nm)

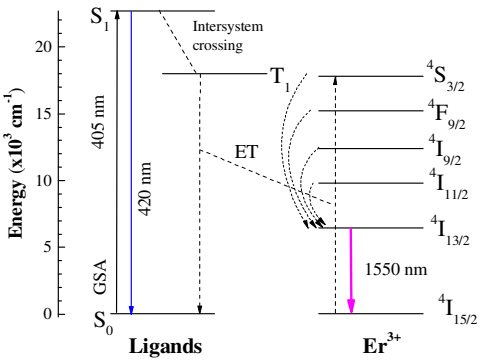

Figure 10. Scheme of the energy transfer mechanism and PL processes

3.8. *Lifetime measurements*

The ligand visible emission and the Er^{3+}:$^4I_{13/2} \rightarrow {}^4I_{15/2}$ transition (1532 nm) decay times are shown in Figure 11 and Figure 12, respectively.

The PL decays of the organic ligands have been measured after excitation with a high-repetition rate pulsed picosecond LED at 280 nm (Figure 11), the same wavelength chosen for the visible PL spectra. The $S_1 \rightarrow S_0$ fluorescence decay was detected at about the maximum of the emission bands. A characteristic non-exponential decay was observed in all the cases due to ligand-to-ligand or ligand-to-metal interactions. In order to estimate an average lifetime, the decay curves were fitted to a three exponential decay curve (equation 1).

$$I(t) = B_1 \cdot e^{(-t/\tau_1)} + B_2 \cdot e^{(-t/\tau_2)} + B_3 \cdot e^{(-t/\tau_3)} \qquad (1)$$

The fitting was made using instrument response function (IRF) reconvolution analysis with FAST® software by Edinburgh Instruments. The average lifetime is then calculated as [16]:

$$\tau_{av} = (B_1\tau_1^2 + B_2\tau_2^2 + B_3\tau_3^2)/(B_1\tau_1 + B_2\tau_2 + B_3\tau_3) \quad (2)$$

The best fitting give an averaged decay of 4.07 ns.

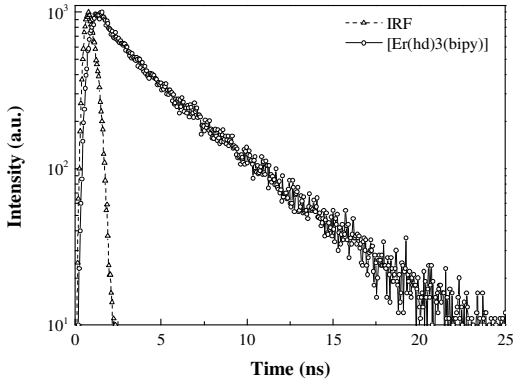

Figure 11. Ligand emission-associated PL decay time in the visible region.

The NIR PL decay of the $^4I_{13/2}$ multiplet was measured after pumping at 980 nm (Figure 12). The decay shows a single exponential behavior, which can be observed as a linear dependence in the semi-log representations in Figure 12. The good fitting to a single-exponential function confirms a unique and consistent coordination environment around the lanthanide ion [17]. The $^4I_{13/2}$ lifetime obtained for the complex, τ=1.05 μs, is quite similar to other Er(III) complexes previously reported [18] and slightly lower than those reported for fluorinated β-diketonate complexes [5,6]. It is probably limited by "second-sphere" matrix interactions.

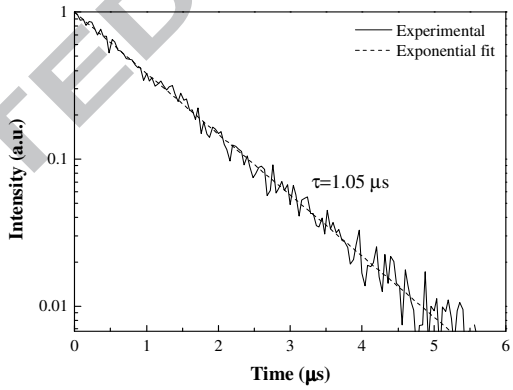

Figure 12. Er^{3+}:$^4I_{13/2}\rightarrow{}^4I_{15/2}$ emission decay

4. Conclusion

A new Er^{3+} complex including negative β-diketonate ligands and a neutral aromatic N,N-donor has been synthesized and its structure determined by X-ray diffraction. Powder diffraction was used to prove the purity of the samples used for photoluminescence studies. The organic ligands have their highest absorption at 292 nm (UV region). When excited in this wavelength region, some residual fluorescent emission from the organic igands appears accompanied with a strong $^4I_{13/2}\rightarrow{}^4I_{15/2}$ emission from Er(III) ion, as a consequence of the so-called "antenna effect". Ligand emission-associated PL decay time in the visible region

confirms the ligand-to-erbium energy transfer, while the erbium(III) $^4I_{13/2}$ lifetime (τ=1.05 μs) is probably limited by "second-sphere" matrix interactions.

5. Acknowledgments

P. Martín-Ramos would like to thank the Spanish Ministry of Education for its financial support and Prof. Dr. Carlos Zaldo for granting access to the ICMM facilities. Prof. Inocencio R. Martín and Prof. Fernando Lahoz are gratefully acknowledged for their insightful comments. CEMDRX group is grateful to Fundação para a Ciência e a Tecnologia (FCT) for providing funds under grant PTDC/FIS/102284/2008. UVa group acknowledges financial support of Junta de Castilla y León through project VA300A12-1.

Appendix A. Supplementary data

CCDC 942390 contains the supplementary crystallographic data for [Er(hd)$_3$(bipy)]. These data can be obtained free of charge via http://www.ccdc.cam.ac.uk/conts/retrieving.html, or from the Cambridge Crystallographic Data Centre, 12 Union Road, Cambridge CB2 1EZ, UK; fax: +44 1223 336 033; or e-mail: deposit@ccdc.cam.ac.uk.

6. References

[1] K. Binnemans, *Chem. Rev.* 109 (2009) 4283–4374; M.A. Katkova, M.N. Bochkarev. *Dalton Trans.* 39 (2010) 6599-6612.
[2] S.V. Eliseeva, J.C.G. Bunzli. *Chem. Soc. Rev.* 39 (2010) 189–227.
[3] J.G. Bunzli, *Acc. Chem. Res.*, 39 (2006) 53-61; J.P. Leonard, T. Gunnlaugsson, *J. Fluoresc.*, 15 (2005) 585-595.
[4] M.A. Katkova, A.P. Pushkarev, T.V. Balashova, A.N. Konev, G.K. Fukin, S.Y. Ketkov, M.N. Bochkarev. *J. Mater. Chem.* 21 (2011) 16611-16620.
[5] P. Martín-Ramos, M. R. Silva, C. Coya, C. Zaldo, A. L. Álvarez, S. Álvarez-García, A. M. Matos Beja, J. Martín-Gil, *J. Mater. Chem. C*, 1 (2013) 2725–2734.
[6] P. Martín-Ramos, C. Coya, A. L. Álvarez, M. R. Silva, C. Zaldo, J. A. Paixão, P. Chamorro-Posada, J. Martín-Gil, *J. Phys. Chem. C*, 117 (2013) 10020–10030.
[7] R. Sabbah, A. Xu-wu, J.S. Chickos, M.L. Planas Leitão, M.V. Roux, L.A. Torres, *Thermochim. Acta*, 331:2 (1999) 93-204.
[8] G. Della Gatta, M.J. Richardson, S.M. Sarge, S. Stolen, *Pure Appl. Chem.*, 78:7 (2006) 1455-1476.
[9] G.M. Sheldrick, *SADABS*. University of Göttingen, Germany, 1996.
[10] G.M. Sheldrick, *SHELXL97 and SHELXS97*. University of Göttingen, Germany, 1997.
[11] A.L. Spek. *J. Appl. Crystallogr.*, 36 (2003) 7-13.
[12] C.K. Pearce, D.W. Grosse, W. Hessel. *Chem. Eng. Data*, 15 (1970) 567-570.
[13] G.B. Deacon, R.I. Phillips. *Coord. Chem. Rev.*, 33:3 (1980) 227–250.
[14] C. Görller-Walrand, K. Binnemans, *Spectral intensities of f-f transitions*, in: K.A. Gschneidner, L. Eyring (Eds.), *Handbook on the physics and chemistry of rare earths, vol. 25, Chapter 167*. Elsevier BV, Amsterdam, 1998.
[15] S.A. Davis, F.S. Richardson. *Inorg. Chem.*, 23 (1984) 184-189.
[16] J.R. Lakowicz, *Principles of Fluorescence Spectroscopy*, Springer, New York, 2010, pp. 141-142.
[17] S. Gajo, J.A. Fernades, J.P. Rainho, R.A. Sá Ferreira, M. Pillinger, A.A. Valente, T.M. Santos, L.D. Carlos, P.J.A. Riberiro-Claro, I.S. Goncualves, *Chem. Mater.*, 17 (2005) 5077-5084.
[18] Z. Li, J. Yu, L. Zhou, H. Zhang, R. Deng, Z. Guo, *Org. Electron.,* 9 (2008) 487-494; X. Li, Z. Si, C. Pan, L. Zhou, Z. Li, X. Li, J. Tang, H. Zhang, *Inorg. Chem. Commun.,* 12 (2009) 675-677.

Figure 1

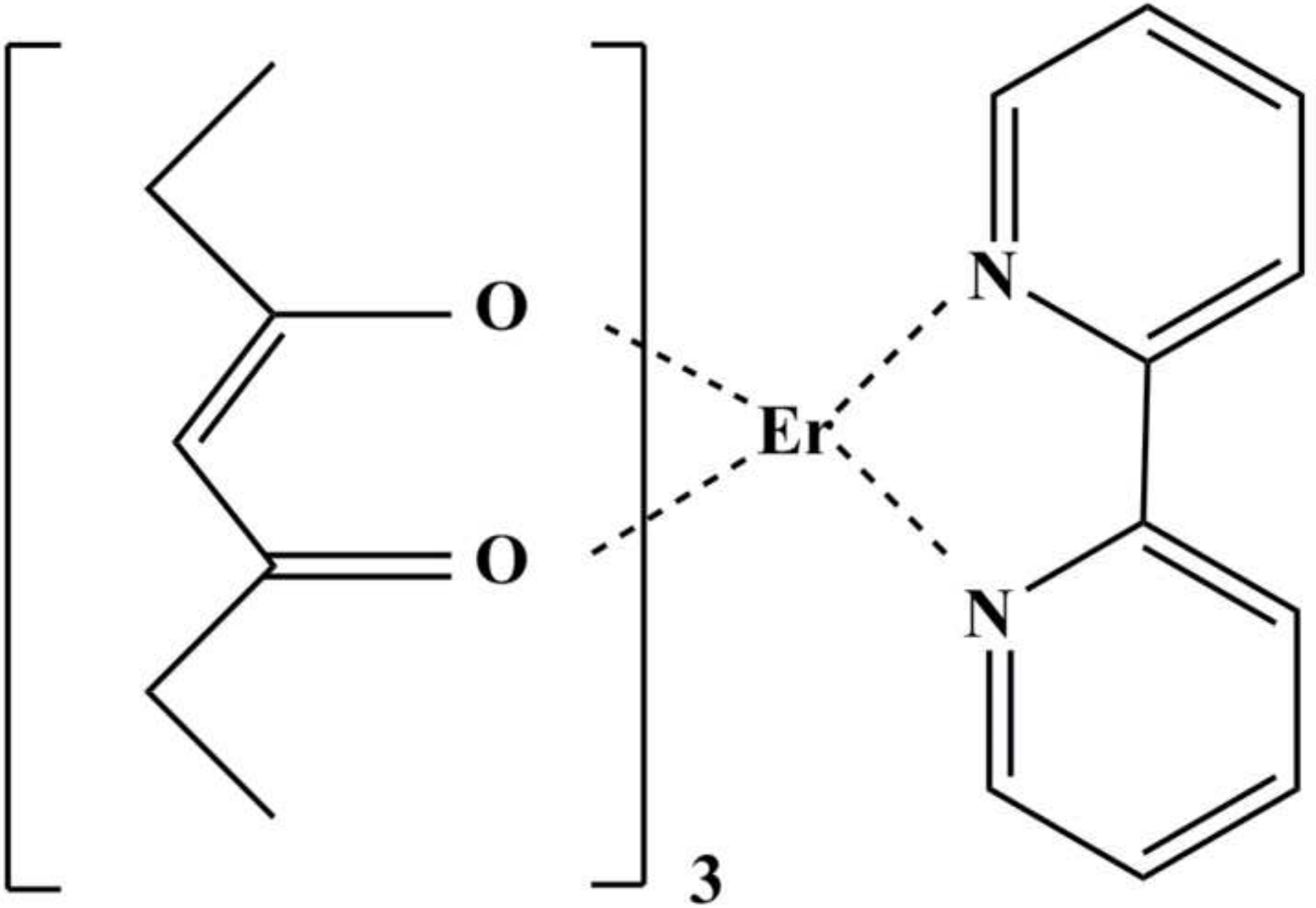

Graphical abstract

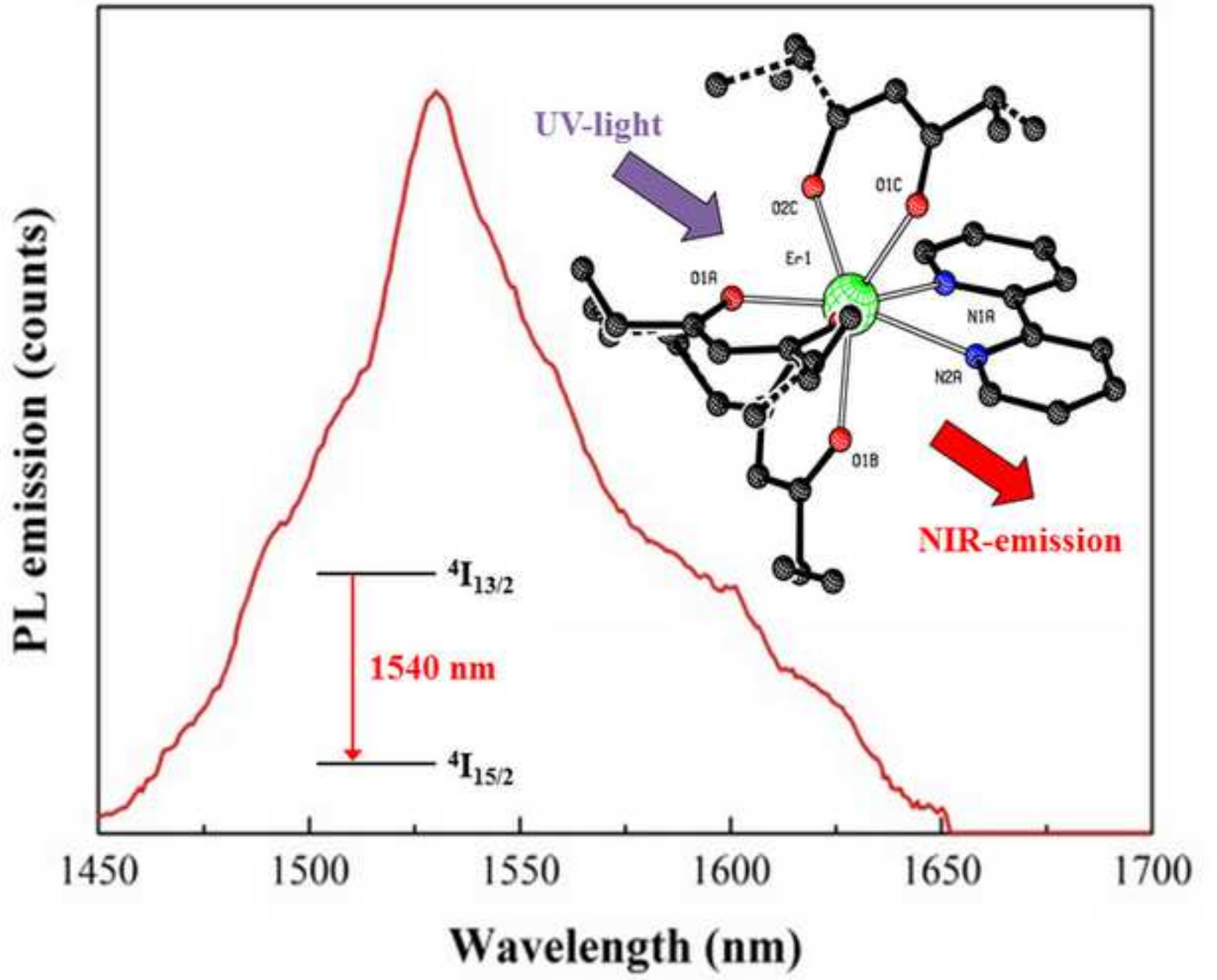

The synthesis and structural elucidation of a new [Er(β-diketonate)$_3$(N,N-donor)] octacoordinated complex are reported, together with calorimetric, FTIR and Raman spectroscopy data and photoluminescent characterization of the material. A significant energy transfer by *antenna effect* from the coordinating ligands to the central Er(III) ion has been confirmed. A potential use of the compound as a NIR emitting material in organic light-emitting devices (OLEDs) is envisaged.